High-pressure Raman spectroscopy of graphene

John E. Proctor,[1,*] Eugene Gregoryanz,[1] Konstantin S. Novoselov,[2] Mustafa Lotya,[3] Jonathan N. Coleman,[3] and Matthew P. Halsall[4]

[1]*School of Physics and Centre for Science at Extreme Conditions, University of Edinburgh, Edinburgh EH9 3JZ, United Kingdom*

[2]*School of Physics and Astronomy, University of Manchester, Oxford Road, Manchester M13 9PL, United Kingdom*

[3]*School of Physics, Trinity College Dublin, Dublin 2, Ireland*

[4]*School of Electrical and Electronic Engineering, Photon Science Institute, University of Manchester, Oxford Road, Manchester M13 9PL, United Kingdom*

(Received 18 May 2009; revised manuscript received 23 July 2009; published 21 August 2009)

In situ high-pressure Raman spectroscopy is used to study monolayer, bilayer, and few-layer graphene samples supported on silicon in a diamond anvil cell to 3.5 GPa. The results show that monolayer graphene adheres to the silicon substrate under compressive stress. A clear trend in this behavior as a function of graphene sample thickness is observed. We also study unsupported graphene samples in a diamond anvil cell to 8 GPa and show that the properties of graphene under compression are intrinsically similar to graphite. Our results demonstrate the differing effects of uniaxial and biaxial strain on the electronic band structure.

DOI: 10.1103/PhysRevB.80.073408 PACS number(s): 68.35.Af, 78.30.Na, 62.25.−g, 62.50.−p

The discovery of graphene in 2004[1] has led to many advances in solid state physics. Research into this new material is fuelled by interest in fundamental physics as the quantum Hall effect has been observed in graphene at room temperature[2] and electrons within graphene behave as massless Dirac fermions, mimicking relativistic particles.[3] Graphene has been suggested as a candidate for a wide variety of applications in electronics (due to its ballistic transport at room temperature) and composite materials.[2] It is the experimental realization of a truly two-dimensional (2D) material.

To date there have been no studies published on graphene at high pressure. This is surprising in view of the huge interest in the mechanical properties of graphene[4–9] motivated particularly by its possible applications in nanoelectronics.[4,5] Strain monitoring is of critical importance[10,11] in this field. It should be of particular relevance in the case of graphene due to the predicted dependence of electronic band gap on strain,[12] and also due to the fact that some of the materials related to graphene are intrinsically stressed due to the presence of the substrate, for example, graphene grown epitaxially on SiC.[13] The possibility of using graphene as an ultrasensitive strain sensor has also been suggested.[9] Study of graphene at high pressure therefore has the potential to develop into an important component in the characterization and understanding of this remarkable new material, as has been the case with carbon nanotubes.

Experiments under hydrostatic pressure have been extensively employed to probe basic characteristics of carbon nanotubes such as compressibility,[14] the nature of the nanotube bundle,[15] and electronic band structure.[16] Further experiments have been motivated by desire to understand the characteristics of composite materials containing nanotubes.[17] The possibilities for using fullerenes and nanotubes for the synthesis of superhard materials at high pressure and temperature, and for hydrogen storage, are also being explored.[18,19]

In this Brief Report we present the study of graphene at high pressure. Samples of monolayer, bilayer, and few-layer graphene supported on silicon are studied, along with unsupported graphene samples. We perform simple calculations to compare our results to those of the recent experiments on graphene under uniaxial strain[8] and the hydrostatic-pressure experiments on graphite.[20,21]

The high-pressure Raman measurements presented in this Brief Report were performed in gasketed symmetric diamond anvil cells (DACs) and recorded using a micro-Raman spectrometer at room temperature. Scattered light from the sample was collected in the backscattering geometry and the 514.5 nm radiation of an Ar^+ laser was used for excitation throughout. The laser power reaching the DAC did not exceed 20 mW. A lower power level (3 mW reaching the sample) was used for spectra taken in air due to the risk of heating and oxidizing the samples. Pressure was recorded using the ruby fluorescence method and nitrogen was used as the pressure-transmitting medium except where otherwise indicated, ensuring quasihydrostatic conditions.

Supported graphene samples were prepared using the mechanical exfoliation technique,[1] on 100-μm-thick silicon wafers coated with a 300-nm-thick SiO_2 layer, and unsupported graphene samples were prepared using the liquid-phase exfoliation technique.[22] The unsupported graphene samples are a mixture of monolayer, bilayer, and few-layer graphene and also contain a small amount of nanographite. Details of the sample preparation are given in the supplementary information.[23]

At low pressures (below $\approx$0.5 GPa) the 2D Raman peak from the graphene samples overlapped partially with the second-order Raman peak from the diamond anvils of the high-pressure cell, so to obtain the 2D Raman peak from the samples we subtracted the background Raman signal from the diamond. See example spectra in the supplementary information.[23]

To complement our experimental data, we perform simple calculations to predict the pressure dependence of the in-plane Raman modes of monolayer graphene. For three-dimensional, isotropic materials the pressure-induced shift of each Raman mode is related to the compression of the material by the mode Grüneisen parameter γ (Ref. 24)

$$\omega(P)/\omega_0 = [V(P)/V_0]^{-\gamma}. \quad (1)$$

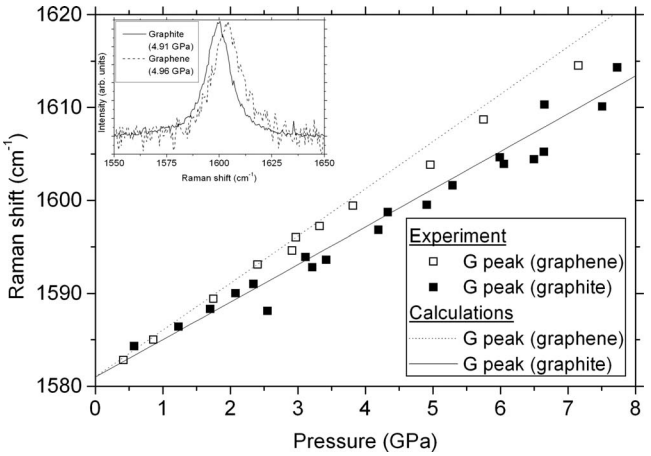

FIG. 1. The evolution of the Raman G peak is shown to 8 GPa for unsupported graphene (open squares) and for graphite (filled squares). The unsupported graphene sample is a mixture of graphene flakes of different thicknesses [see supplementary information (Ref. 23)]. Our calculations are shown for graphene (dotted line) and graphite (continuous line) using the Grüneisen parameters measured experimentally in Refs. 8 and 20, respectively, and Eq. (2). Inset shows example spectra at 5 GPa.

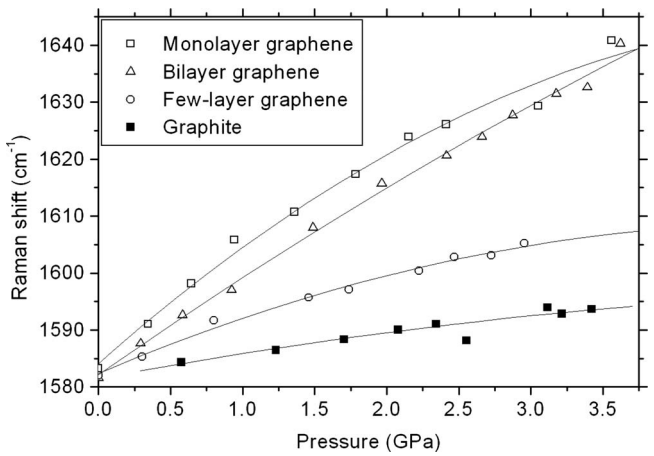

FIG. 2. The evolution of the Raman G peak is shown to ≈3.5 GPa for monolayer (open squares), bilayer (open triangles), and few-layer (open circles) graphene on silicon and free-standing graphite (filled squares, the same sample and data as in Fig. 1). Our results for free-standing graphite are virtually identical to those we obtain for graphite on silicon (see Fig. 3). Lines are polynomial fits, intended only as guides to the eye.

However, in graphite the in-plane compressibility (a axis) is an order of magnitude lower than the out-of-plane compressibility (c axis)[20] so it is preferable to define Grüneisen parameters for the in-plane and out-of-plane vibrational modes separately using the linear compressibility along the a and c axes, respectively. For the in-plane E_{2g} mode at 1580 cm^{-1} under hydrostatic pressure or in-plane biaxial compression one should write

$$\omega(P)/\omega_0 = [a(P)/a_0]^{-2\gamma_{E_{2g}}}. \quad (2)$$

For uniaxial compression one should write

$$\omega(P)/\omega_0 = [a(P)/a_0]^{-\gamma_{E_{2g}}}. \quad (3)$$

This follows the approach of Refs. 20 and 25 and is the definition used in the investigations of graphene under uniaxial strain in Ref. 8 where the Grüneisen parameters are calculated for the E_{2g} (G peak, 1583 cm^{-1}) and A_{1g} (2D peak, 2680 cm^{-1}) in-plane Raman modes of graphene. Assuming that the in-plane compressibility of graphene is the same as for graphite (given in Ref. 20) we can use Eq. (2) with the Grüneisen parameters calculated for graphene in Ref. 8 to predict the pressure-induced shifts of the in-plane Raman modes of unsupported graphene.

Figure 1 shows the evolution of the G peak of unsupported graphene samples to 8 GPa, with our results for graphite shown for comparison. We observe a slightly larger shift of the graphene G peak to higher wave numbers at pressure than is the case for graphite. Also in Fig. 1, we calculate the pressure-induced shift of the G peak using the Grüneisen parameter for graphene obtained from the uniaxial strain experiments of Ref. 8 ($\gamma_{E_{2g}}=1.99$, in excellent agreement with the DFT calculations conducted in Ref. 26 prior to the experimental discovery of graphene), and using the Grüneisen parameter for graphite from Ref. 20 [$\gamma_{E_{2g}}=1.59$ using the definition of Eq. (2)]. We find good agreement with the experimental data for graphene and graphite, respectively. The small difference in behavior between graphene and graphite observed in Fig. 1 is not necessarily mechanical in origin. It could be due to some chemical interaction between the graphene and the pressure-transmitting medium. Several studies have noted these effects in carbon nanotubes at high pressure, for example, molecular organization of the pressure-transmitting medium molecules around the nanotubes[27] and doping of the nanotubes[28] have small effects on the observed Raman spectra at high pressure. In any case, the reported pressure-induced shifts of the Raman G peak for graphite vary, ranging from 4.1 (Ref. 29) to 4.7 (Ref. 20) cm^{-1} GPa^{-1}.

In Fig. 2 we show our data for the Raman G peak of monolayer, bilayer, and few-layer graphene on silicon and free-standing graphite. A clear trend is observed that the shift of the G peak to higher wave number with applied pressure is larger for thinner flakes of graphene. We observe the same trend for the 2D peak (see supplementary material[23]). To confirm this trend we loaded a sample of graphene on silicon containing two flakes of different thicknesses into the diamond anvil cell simultaneously (Fig. 3). The Raman G peak from the flake that was visibly thicker (see photograph in the inset) shifted to higher wave numbers at a slower rate with applied pressure. Figure 3 also shows our data for the Raman G peak of a thin layer of graphite on silicon deposited using the same mechanical exfoliation technique as is used for the graphene samples, and for free-standing graphite. The observed pressure-induced Raman shifts for the supported and free-standing graphite are found to be very similar.

Our calculations of the pressure-induced shifts of the graphene Raman peaks [Eqs. (1) and (2)] can be extended to the case of graphene on the silicon/SiO_2 substrate. In these calculations, we assume that the graphene, SiO_2 and silicon remain bonded. The silicon layer is 100 μm thick, the SiO_2

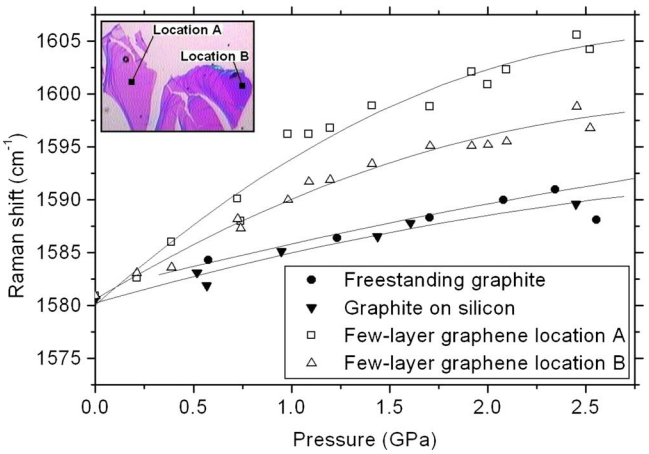

FIG. 3. (Color online) The evolution of the Raman G peak is shown for the few-layer graphene flakes of different thicknesses on silicon shown in the inset (the flake at location B was thicker than at location A, shown in color online). For comparison, data for free-standing graphite and graphite on silicon are presented. Data for graphene and graphite on silicon in this figure were taken with 4:1 methanol-ethanol solution as pressure-transmitting medium. Lines are polynomial fits, intended only as guides to the eye.

layer is 300 nm thick, and the graphene layer is <1 nm thick. We adopt the approach used in the extensive literature on the fabrication and high-pressure study of III-V and II-VI semiconductor materials grown epitaxially on a substrate. If the epilayer is sufficiently thin compared to the substrate, it is assumed that the compression of the entire sample is determined by the compressibility of the substrate. See, for example, Refs. 30 and 31. We therefore assume that the compression of our sample is determined by the compressibility of the silicon substrate. We derive the linear compressibility of silicon at low pressure from the bulk modulus. The bulk modulus B_0 is related to the compression of the Si-Si bonds as follows:

$$B_0 = -V\frac{dP}{dV} \tag{4}$$

$$V(P) = V_0\left(\frac{r(P)}{r_0}\right)^3. \tag{5}$$

The Si-Si bond length at zero pressure is r_0 and at arbitrary pressure $r(P)$. From Eqs. (4) and (5) we can derive an approximate relation for the linear compressibility at low pressure and use the bulk modulus from Ref. 32, B_0 =97.88 GPa, to calculate it's value.

$$\frac{d}{dP}\left(\frac{r}{r_0}\right) \approx \frac{1}{3B_0} \approx 0.0034 \text{ GPa}^{-1}. \tag{6}$$

In Eq. (2) the pressure-induced shifts of the intralayer Raman modes of free-standing graphene are calculated from the in-plane compression of the graphene sample as a function of pressure ($\frac{a(P)}{a_0}$). To calculate the pressure-induced shifts of the intralayer Raman modes of graphene on the silicon substrate we substitute the compression of the silicon substrate $\frac{r(P)}{r_0}$ for $\frac{a(P)}{a_0}$ in Eq. (2). The absolute values of a_0 and r_0 are not used in the calculation, so the fact that graphene has a different lattice constant to silicon is not relevant. The only assumption we make is that the graphene adheres to the substrate, i.e., if at a given pressure the silicon substrate contracts to 95% of it's diameter at 0 GPa then the graphene sample will also contract to 95% of it's diameter at 0 GPa. This is the only assumption that is necessary to replace $\frac{a(P)}{a_0}$ with $\frac{r(P)}{r_0}$ in Eq. (2) for the case of graphene on silicon. The linear compressibility of silicon determined in Eq. (6) is then used to calculate $\frac{r(P)}{r_0}$ as a function of P.

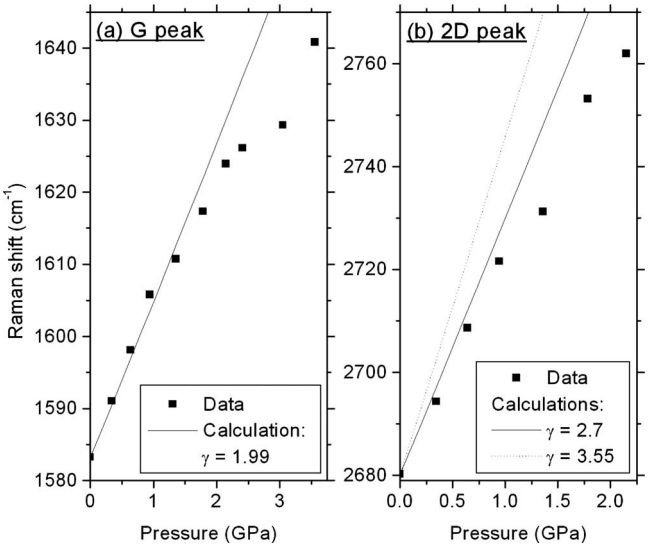

FIG. 4. The evolution of the (a) G and (b) 2D Raman peaks for monolayer graphene on silicon are shown to 3.6 and 2.3 GPa, respectively, (black squares). In (a), the solid line is the calculated Raman shift for monolayer graphene adhering perfectly to a silicon substrate using the Grüneisen parameter obtained from recent investigations on graphene under uniaxial strain (Ref. 8) ($\gamma_{E_{2g}}$ =1.99). In (b), the solid line is the calculated Raman shift using the Grüneisen parameter obtained from the density-functional theory calculations for graphene (Ref. 8) ($\gamma_{A_{1g}}$=2.7), and the dashed line is the calculated Raman shift using the Grüneisen parameter obtained from the investigations on graphene under uniaxial strain (Ref. 8) ($\gamma_{A_{1g}}$=3.55).

In Fig. 4 we compare our data for the G and 2D peaks of monolayer graphene on silicon to our calculations using the Grüneisen parameters obtained in recent experiments on graphene under uniaxial strain.[8] At lower pressures, we find good agreement in the case of the G peak. However, in the case of the 2D peak our results show better agreement with those on graphite under hydrostatic pressure[21] ($\gamma_{A_{1g}}$=2.84) and with those of the density-functional theory calculations for graphene[8] ($\gamma_{A_{1g}}$=2.7) than with those of the uniaxial strain experiments on graphene ($\gamma_{A_{1g}}$=3.55). However, as discussed in Ref. 8, this can be explained by the origin of the 2D Raman peak in a double resonance Raman process. In an experiment under uniaxial strain, the relative positions of the Dirac cones in the graphene electronic band structure are changed, so the double resonance condition and actual phonon probed in the Raman measurements will also change. However, in our experiments the in-plane compression is bi-

axial and the effects due to the relative movement of the Dirac cones are absent. This is why our data are in agreement with the hydrostatic pressure experiments on graphite[21] instead of the experiments on graphene under uniaxial strain.[8]

At higher pressures, both the *G* and 2D Raman peaks shift to higher wave numbers with applied pressure at a lower rate than predicted. This could be due to debonding between the different layers of our sample (graphene, SiO_2, and silicon). Since the SiO_2 and silicon are covalently bonded while the graphene is attached to the SiO_2 only by Van der Waal's forces, poor adherence between the graphene and the SiO_2 at higher pressures is most likely. Using Eq. (6) we see that 2 GPa corresponds to a compressive biaxial strain of 0.68% for the graphene on silicon/SiO_2. Alternatively, as discussed earlier, chemical interactions between the graphene and pressure-transmitting medium could play a role. However, our results for unsupported graphene at high pressure are similar to those for graphite, and the results of our experiments using 4:1 methanol ethanol as pressure-transmitting medium (Fig. 3) are qualitatively the same as those with nitrogen (Figs. 1, 2, and 4), so the role played by any chemical interactions between the graphene and the pressure-transmitting media must be small.

Our data on few-layer graphene displays a clear trend, that the pressure-induced shifts of the *G* and 2D Raman peaks are larger for thinner samples. This suggests that thicker samples do not adhere as well to the substrate under compressive stress as a monolayer. It is interesting to note that the low-pressure compressibility of materials could, in principle, be measured using only optical spectroscopy by depositing a monolayer of graphene on the surface of the material, and using Raman spectroscopy of the monolayer to measure the strain in the material under investigation.

In conclusion, we have studied graphene at high pressure in order to confirm key mechanical characteristics of the material. These are needed due to its potential applications in nanoelectronics, in which the intentional use of strain could improve device characteristics, and the current interest in intrinsically stressed graphene samples, such as graphene grown epitaxially on SiC. Our work is in agreement with the uniaxial strain study of Mohiuddin *et al.*[8] in finding that the strain dependences of the in-plane phonon frequencies (as determined by the Grüneisen parameter) are similar to those for graphite, and in disagreement with the uniaxial strain studies that suggest they are significantly smaller than for graphite.[33,34] Our comparison of supported and unsupported graphene samples demonstrates that the compression of the graphene is initially (i.e., at low pressures) determined by the compressibility of the substrate. The good adherence of monolayer graphene to the Si/SiO_2 substrates in our experiments under hydrostatic pressure, and to the polydimethylsiloxane, polyethylene terephthalate, and perspex substrates in the recent uniaxial strain experiments,[4,8] demonstrates the potential application of graphene as a strain sensor.

The authors would like to acknowledge the help of Malachy McGowan (School of Electrical and Electronic Engineering, University of Manchester) in the preparation of the graphene samples. We would also like to thank Chrystéle Sanloup (School of Geosciences, University of Edinburgh) and David Dunstan (Physics Deptartment, Queen Mary, University of London) for advice about the calculations. This work was supported by a research grant from the U.K. Engineering and Physical Sciences Research Council.

*Corresponding author. jproctor@staffmail.ed.ac.uk

[1] K. S. Novoselov *et al.*, Science **306**, 666 (2004).
[2] A. K. Geim and K. S. Novoselov, Nature Mater. **6**, 183 (2007).
[3] C. W. J. Beenakker, Rev. Mod. Phys. **80**, 1337 (2008).
[4] K. S. Kim *et al.*, Nature (London) **457**, 706 (2009).
[5] V. M. Pereira and A. H. Castro Neto, Phys. Rev. Lett. **103**, 046801 (2009).
[6] C. Lee *et al.*, Science **321**, 385 (2008).
[7] J. Zhou and R. Huang, J. Mech. Phys. Solids **56**, 1609 (2008).
[8] T. M. G. Mohiuddin *et al.*, Phys. Rev. B **79**, 205433 (2009).
[9] T. Yu *et al.*, J. Phys. Chem. C **112**, 12602 (2008).
[10] A. Ourmazd, Nat. Nanotechnol. **3**, 381 (2008).
[11] M. Hÿtch *et al.*, Nature (London) **453**, 1086 (2008).
[12] G. Gui *et al.*, Phys. Rev. B **78**, 075435 (2008).
[13] J. Röhrl *et al.*, Appl. Phys. Lett. **92**, 201918 (2008).
[14] S. M. Sharma *et al.*, Phys. Rev. B **63**, 205417 (2001).
[15] U. D. Venkateswaran *et al.*, Phys. Rev. B **59**, 10928 (1999).
[16] S. Lebedkin *et al.*, Phys. Rev. B **73**, 094109 (2006).
[17] J. R. Wood *et al.*, Phys. Rev. B **62**, 7571 (2000).
[18] I. Loa, J. Raman Spectrosc. **34**, 611 (2003).
[19] C. Liu *et al.*, Science **286**, 1127 (1999).
[20] M. Hanfland *et al.*, Phys. Rev. B **39**, 12598 (1989).
[21] A. F. Goncharov, JETP Lett. **51**, 418 (1990).
[22] Y. Hernandez *et al.*, Nat. Nanotechnol. **3**, 563 (2008).
[23] See EPAPS Document No. E-PRBMDO-80-070931 for details of sample preparation techniques, example Raman spectra at ambient pressure and high pressure, and evolution of the Raman 2D peak at high pressure for various samples. For more information on EPAPS, see http://www.aip.org/pubservs/epaps.html.
[24] B. Weinstein and R. Zallen, in *Light Scattering in Solids*, edited by M. Cardona and G. Güntherodt (Springer, Berlin, 1984), Vol. IV.
[25] R. Zallen, Phys. Rev. B **9**, 4485 (1974).
[26] C. Thomsen *et al.*, Phys. Rev. B **65**, 073403 (2002).
[27] P. Puech *et al.*, Phys. Rev. B **73**, 233408 (2006).
[28] P. Puech *et al.*, Phys. Rev. B **78**, 045413 (2008).
[29] L. Zhenxian *et al.*, J. Phys. Condens. Matter **2**, 8083 (1990).
[30] E. P. O'Reilly, Semicond. Sci. Technol. **4**, 121 (1989).
[31] V. A. Wilkinson *et al.*, Phys. Rev. B **42**, 3113 (1990).
[32] J. Z. Hu *et al.*, Phys. Rev. B **34**, 4679 (1986).
[33] M. Huang *et al.*, Proc. Natl. Acad. Sci. U.S.A. **106**, 7304 (2009).
[34] Z. H. Ni *et al.*, ACS Nano **2**, 2301 (2008).